ARTHRITIS & RHEUMATOLOGY
Vol. 68, No. 1, January 2016, pp 138–151
DOI 10.1002/art.39425

Inhibition of Osteoarthritis by Adipose-Derived Stromal Cells Overexpressing Fra-1 in Mice

Kay Schwabe,[1] Mireia Garcia,[1] Kenia Ubieta,[1] Nicole Hannemann,[1] Bettina Herbort,[1] Julia Luther,[2] Daniele Noël,[3] Christian Jorgensen,[3] Louis Casteilla,[4] Jean-Pierre David,[2] Michael Stock,[1] Martin Herrmann,[1] Georg Schett,[1] and Aline Bozec[1]

Objective. **To determine whether overexpression of the activator protein 1 (AP-1) transcription factor Fra-1 in adipose-derived stromal cells (ADSCs) is an effective treatment of collagenase-induced osteoarthritis (OA).**

Methods. **OA was induced by injection of collagenase into the knee joints of male C57BL/6 mice. ADSCs were isolated from the inguinal fat pads of 8-week-old wild-type or Fra-1–transgenic mice and injected into the knee joints of mice with collagenase-induced OA 7 days after OA induction. Histologic analyses of cartilage destruction and chondrocyte cell death were performed. Adipogenic differentiation capacity was evaluated, gene expression was analyzed, and cytokine profiling was performed in stromal vascular fractions (SVFs) and ADSCs.**

Results. **OA-related cartilage destruction and chondrocyte cell death were significantly reduced in mouse knee joints treated with ADSCs from Fra-1–transgenic mice compared to mouse knee joints treated with ADSCs from wild-type mice. This effect did not result from the higher number of adipogenic progenitors observed in SVFs from Fra-1–transgenic compared to wild-type mouse fat pads, since injection of wild-type mouse ADSCs enriched for adipogenic progenitors did not show any additional chondroprotective effects compared to nonsorted ADSCs. However, Fra-1–transgenic mouse ADSCs showed decreased adipogenic differentiation capacity. Moreover, Fra-1 significantly inhibited proinflammatory interleukin-6 and pentraxin 3 expression, while increasing the expression of extracellular matrix proteins, such as periostin and spondin 1. These findings suggest that Fra-1 overexpression leads to an increased chondroprotective effect of ADSCs in OA.**

Conclusion. **ADSCs overexpressing Fra-1 effectively protect against OA. Our data indicate that genetic modifications of ADSCs, such as Fra-1 overexpression, may improve their potential to protect articular cartilage against OA-mediated damage.**

Osteoarthritis (OA) is the most common rheumatic disease, characterized by degeneration of articular cartilage. OA patients experience intense pain and impaired physical function. The high prevalence of OA, along with the severe disease burden, is also associated with high socioeconomic costs and loss of productivity (1,2). Mechanistically, it is thought that the balance between anabolic and catabolic factors in cartilage is disturbed, leading to a catabolic phenotype of articular chondrocytes. Different primary triggers eventually lead to a decrease in the capacity of chondrocytes to secrete specific components of the extracellular matrix, such as type IIB collagen or aggrecan, while at the same time the synthesis of catabolic enzymes, such as aggrecanases of the ADAMTS family and collagenases of the matrix

Supported by the DFG (Emmy Noether Programme grant) and the European Union (Seventh Framework Programme projects Adipoa, Masterswitch, and Marie Curie ITN Osteoimmune, and the Innovative Medicines Initiative project BTCure).

[1]Kay Schwabe, MSc, Mireia Garcia, PhD, Kenia Ubieta, MSc, Nicole Hannemann, MSc, Bettina Herbort, PhD, Michael Stock, PhD, Martin Herrmann, PhD, Georg Schett, MD, Aline Bozec, PhD: University of Erlangen–Nuremberg, Erlangen, Germany; [2]Julia Luther, PhD, Jean-Pierre David, PhD: University of Erlangen–Nuremberg, Erlangen, Germany, and University Medical Center Hamburg–Eppendorf, Hamburg, Germany; [3]Daniele Noël, PhD, Christian Jorgensen, MD, PhD: INSERM U844, Hôpital Saint-Eloi, Montpellier, France; [4]Louis Casteilla, PhD: INSERM U1031, STROMALab, Universite Paul Sabatier, CNRS-EFS-UMR5273, Toulouse, France.

Address correspondence to Aline Bozec, PhD, Department of Internal Medicine 3, Rheumatology and Immunology, University of Erlangen–Nuremberg, Ulmenweg 18, Erlangen D-91054, Germany. E-mail: aline.bozec@uk-erlangen.de.

Submitted for publication July 30, 2014; accepted in revised form September 1, 2015.

metalloproteinase (MMP) family, increases (3,4). These catabolic effects are further aggravated by a higher rate of chondrocyte cell death and increased production of proinflammatory cytokines (e.g., interleukin-1β [IL-1β], IL-6, and tumor necrosis factor [TNF]) by synoviocytes and chondrocytes, promoting the production of proteinases, prostaglandins, and nitric oxide (5). To date no treatment has been developed that is actually capable of altering the progression of OA. Furthermore, therapeutic options are limited to the management of inflammation and pain as well as surgical intervention (6,7).

Apart from new drugs, stem cell–mediated approaches to treatment have been studied, mainly using mesenchymal stem cells (MSCs) from the bone marrow or adipose-derived stromal cells (ADSCs) from the adipose tissue. Both cell types are able to self-renew and are capable of differentiating toward chondrocytes, osteoblasts, and adipocytes (8). The number of MSCs derived from the bone marrow is very low compared to the number of ADSCs. It has been calculated that in adipose tissue up to 5% of all nucleated cells in the stromal vascular fraction (SVF) are ADSCs, whereas in the bone marrow only 0.0001–0.01% of the nucleated cells are MSCs (9). In addition, the isolation of ADSCs is easily feasible by liposuction, making ADSCs of particular interest as an instrument for OA treatment. Recently, it has been shown that intraarticular injections of ADSCs in mouse and rabbit models of OA reduced disease severity by inducing antiinflammatory responses and chondroprotective effects (10,11). However, the beneficial effects of ADSCs could possibly be improved by the use of genetically modified ADSCs with enhanced antiinflammatory and/or chondroprotective potential.

Activator protein 1 (AP-1) transcription factors act as sensors of the cellular microenvironment, inducing proliferative, apoptotic, or differentiating signals. Since AP-1 is known to control the development of mesenchymal tissue (12), we hypothesized that ADSCs overexpressing Fra-1 (a Fos member of the AP-1 family) might have a beneficial effect in OA. Fra-1 regulates matrix Gla protein (MGP) in osteoblastic cells (13), and its overexpression blocks adipocyte differentiation (14), suggesting that Fra-1–transgenic mouse ADSCs may retain their progenitor properties. Finally, Fra-1 can negatively regulate the expression of proinflammatory cytokines such as TNF and IL-1β (15,16). Therefore, Fra-1 is an interesting candidate for fostering the protective effects of ADSCs during OA.

In the present study, we show that Fra-1 overexpression in ADSCs indeed changes the expression pattern of secreted proteins in ADSCs, leading to decreased IL-6, pentraxin 3 (PTX3), and plasminogen activator inhibitor 1 (PAI-1) production and increased periostin and spondin 1 expression. Most importantly, we provide evidence that ADSCs overexpressing Fra-1 possess an elevated potential to convey cartilage protection in an experimental OA model.

MATERIALS AND METHODS

Animals. C57BL/6 mice were obtained from Charles River. Male mice were evaluated at ages 8–12 weeks and received a standard diet and tap water ad libitum. Fra-1–transgenic mice ubiquitously overexpress the transcription factor Fra-1 (Fra-1–transgenic mice on a C57BL/6 background) and have been described previously (17). The local ethics committee of the University of Erlangen–Nuremberg approved all experimental procedures.

Adipose-derived stromal cells. ADSCs were isolated from adipose tissue surrounding the inguinal lymph nodes of 8-week-old female mice as previously described (18). They were cultured until the end of passage 1 according to standard procedures in Dulbecco's modified Eagle's medium (DMEM)–Ham's F-12 (Gibco) supplemented with 10% newborn calf serum (NCS; Sigma-Aldrich), 1% penicillin/streptomycin (Invitrogen), 0.5% amphotericin B (Invitrogen), 16 μM biotin (Sigma-Aldrich), 18 μM pantothenic acid (Sigma-Aldrich), and 100 μM ascorbic acid (Sigma-Aldrich). A total of 20,000 ADSCs (passage 1) in 6 μl of mouse serum (Sigma-Aldrich) were injected intraarticularly into the mouse knee joint. Control mice were injected with mouse serum only (Figure 1A).

For short hairpin RNA (shRNA) transfection, ADSCs (passage 1) were cultured in 6-well plates until they reached 70–80% confluence. Cells were transfected with 1 μg per well of periostin shRNA plasmid (Santa Cruz Biotechnology) or green fluorescent protein–expressing control plasmid using Lipofectamine transfection reagent according to the recommendations of the manufacturer (Life Technologies). The transfected cells were incubated at 37°C in 5% CO_2 for 3 days.

For differentiation studies, ADSCs (passage 1) were plated at a density of 4,000 cells/cm^2 (adipogenesis) or 20,000 cells/cm^2 (chondrogenesis). When cells reached confluence, adipogenic differentiation was induced by the addition of medium with 5 μg/ml insulin, 1 μM dexamethasone, and 5 μM 3-isobutyl-1-methylxanthine (Sigma-Aldrich). Chondrogenic differentiation was induced by supplementing medium with 50 mM L-ascorbic acid 2-phosphate, $10^{-8} M$ dexamethasone, 1× insulin–transferrin–selenium (Sigma-Aldrich), and 10 ng/ml of transforming growth factor β3 (TGFβ3; Life Technologies).

For stimulation experiments, confluent ADSC cultures were starved for 6 hours in medium with 0.5% NCS and then stimulated with 10 nM recombinant leptin (Biomol) or 10% NCS for the indicated periods. To study inflammatory responses, confluent ADSC cultures were stimulated with 10 ng/ml of lipopolysaccharide (LPS) for the indicated times.

Induction of OA. Experimental collagenase-induced OA was induced as previously described (19). Briefly, the knee joints of mice were injected with 1 unit of type VII collagenase from *Clostridium histolyticum* (Sigma-Aldrich) dissolved in 5 μl of phosphate buffered saline (PBS) on days 0 and 2, respectively. Mice were evaluated on day 42 after induction of OA (Figure 1A). In this model, which is characterized by OA-like cartilage damage, the injected collagenase does not directly

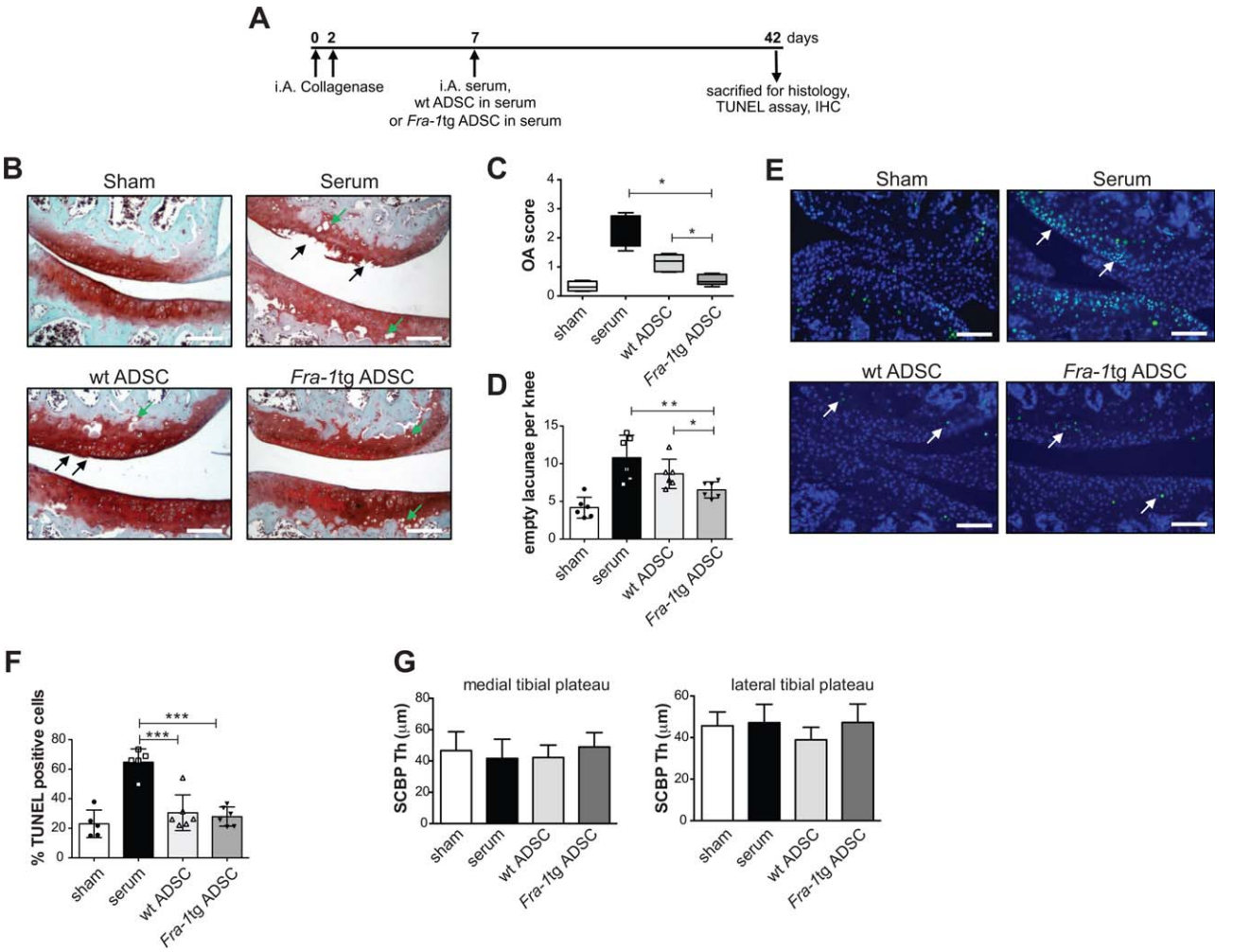

Figure 1. Increased chondroprotective effects of Fra-1–transgenic (Fra-1Tg) mouse adipose-derived stromal cells (ADSCs) in collagenase-induced osteoarthritis (OA). **A,** Schematic illustration of the schedule of induction of collagenase-induced OA in mice and treatment with wild-type (WT) and Fra-1–transgenic mouse ADSCs. IA = intraarticular; IHC = immunohistochemical analysis. **B,** Safranin O–fast green–stained frontal knee joint sections from control mice without OA (sham) and mice with OA that were injected with serum, wild-type mouse ADSCs, or Fra-1–transgenic mouse ADSCs. **Black arrows** indicate cartilage lesions. **Green arrows** indicate empty chondrocyte lacunae. **C** and **D,** Quantification of cartilage damage (**C**) and mean number of empty chondrocyte lacunae per knee joint (**D**) in control mice without OA and mice with OA that were injected with serum, wild-type mouse ADSCs, or Fra-1–transgenic mouse ADSCs. Data in **C** are shown as box plots. Each box represents the 25th to 75th percentiles. Lines inside the boxes represent the mean. Lines outside the boxes represent the 10th and 90th percentiles. Bars in **D** show the mean ± SEM. Symbols represent individual mice (n = 6 mice per group). **E** and **F,** TUNEL staining (**E**) and mean percentage of TUNEL-positive cells (**F**) in knee joint sections from control mice without OA and mice with OA that were injected with serum, wild-type mouse ADSCs, or Fra-1–transgenic mouse ADSCs. **Arrows** indicate TUNEL-positive cells. Bars in **F** shows the mean ± SEM. Symbols represent individual mice (n = 6 mice per group). **G,** Subchondral bone thickness (SCBP Th) quantification at the medial and lateral tibial plateaus in control mice without OA and mice with OA that were injected with serum, wild-type mouse ADSCs, or Fra-1–transgenic mouse ADSCs. Values are the mean ± SEM. Bars in **B** and **E** = 100 μm. * = $P < 0.05$; ** = $P < 0.001$; *** = $P < 0.0001$.

digest cartilage but causes instability of the joints by damaging ligaments (20,21).

Histologic analysis of OA. Mouse knee joints were dissected and fixed in 4% formalin. After fixation, the joints were decalcified in 14% EDTA and processed for histologic analysis. The starting point for the collection of frontal anterior serial sections was the disappearance of the infrapatellar fat pad tissue and the appearance of femoral and tibial plateaus. Serial sections (2 μm each) were collected on glass slides until loss of cartilage on the tibia and/or appearance of synovial tissue in the joint space. A minimum of 10 sections per joint, distributed over the entire joint, were stained with Safranin O–fast green for analysis of cartilage damage and empty chondrocyte lacunae.

In the collagenase-induced OA model, cartilage fibrillation and lesions were observed and scored using a modified form of the OA Research Society International (OARSI) grading system for histopathologic assessment of OA cartilage

(22). The depth of the cartilage damage as well as the extent of the damaged surface were scored in a blinded manner at 4 different locations in the mouse knee joint, i.e., the lateral and medial tibia and femur, using an arbitrary grading scale of 0–6 for the severity of cartilage destruction and of 0–5 for the extent of damaged cartilage surface (stage). Average grades of 5 sections per joint were then multiplied with average stage to determine the OA score per location. The average of these location scores represented the mean OA score per knee joint. Empty cartilage lacunae, indicating chondrocyte cell death, were counted in the cartilage plateaus of the 4 different joint regions. A TUNEL assay was performed according to the manufacturer's instructions (Roche). Slides were mounted in Vectashield mounting media with DAPI and analyzed on a fluorescence microscope. Immunohistochemical staining for IL-6 (Santa Cruz Biotechnology) was performed on paraffin sections using a Vectastain kit according to the instructions of the manufacturer (Vector).

Analysis and sorting of SVFs. SVFs were analyzed by fluorescence-activated cell sorting (FACS) as previously described (23). Briefly, isolated SVFs were resuspended in ice-cold DMEM or magnetic-activated cell sorting (MACS) buffer supplemented with 2% FCS and stained for 15 minutes on ice with phycoerythrin (PE)–Cy7–conjugated CD31, allophycocyanin (APC)–eFluor780–conjugated CD45, APC–eFluor780–conjugated TER119, APC-conjugated CD29, eFluor450-conjugated CD34, fluorescein isothiocyanate (FITC)–conjugated Sca-1, and PE-conjugated CD24 (eBioscience). Cells were centrifuged and resuspended in fresh MACS buffer. Samples were analyzed by a Gallios flow cytometer (Beckman Coulter), equipped with Kaluza analysis software, or sorted by a MoFlo Legacy cell sorter (Beckman Coulter).

Flow cytometric analysis of apoptosis. Apoptosis and necrosis were quantified in confluent ADSCs (passage 1) by FITC-conjugated annexin V (Life Technologies) staining in the presence of TO-PRO-3 iodide (Life Technologies). Detached ADSCs were incubated for 15 minutes at room temperature with 200 μl of FITC-conjugated annexin V in annexin V binding buffer, washed, and resuspended in 200 μl of annexin binding buffer together with TO-PRO-3 iodide. Stained cells were then analyzed by flow cytometry (FACSCalibur; BD Biosciences).

Quantitative reverse transcriptase–polymerase chain reaction (qRT-PCR). Total RNA was extracted using a combination of TriFast reagent according to the recommendations of the manufacturer (PeqLab). Residual genomic DNA was digested with DNase I (Fermentas), and purified RNA was used for the synthesis of complementary DNA (cDNA) with a reverse transcription system kit (Applied Biosystems). In all assays, cDNA was amplified using a standardized program. Real-time qRT-PCR was performed using a SYBR Green kit (Eurogentec) for amplification in a LightCycler system (Applied Biosystems). Analysis of dissociation curves was carried out to exclude artifacts resulting from nonspecific amplification (e.g., primer dimers). Relative quantification was performed after normalization to multiple housekeeping genes (HPRT, GAPDH, and actin) using the $\Delta\Delta C_t$ method. In the figures, qRT-PCR representative graphs are presented with relative expression normalized to that of HPRT. The following primers were used for real-time qPCR analyses: for HPRT, forward GTTAAGCAGTACAGCCCCAAA and reverse AGGGCATATCCAACAACAAACTT; for GAPDH, forward CTACACTGAGGACCAGGTTGTCT and reverse CAGGAAATGAGCTTGACAAAGTT; for actin, forward TGTCCACCTTCCAGCAGATGT and reverse AGCTCAGTAACAGTCCGCCTAGA; for Fra-1, forward GAGACGCGAGCGGAACAAG and reverse CTTCCAGCACCAGCTCAAGG; for peroxisome proliferator–activated receptor 2 (PPARγ2), forward CTGATGCACTGCCTATGAGC and reverse GGGTCAGCTCTTGTGAATGG; for CCAAT/enhancer binding protein α (C/EBPα), forward TGGACAAGAACAGCAACGAG and reverse CTGGTCAACTCCAGCACCTT; for C/EBPβ, forward TTTCGGGACTTGATGCAATC and reverse CCGCAGGAACATCTTTAAGG; for C/EBPδ, forward GAACACGGGAAAGCATGACT and reverse CTTCGGCAACCACCTAAAAG; for glucose transporter 4 (GLUT-4), forward GAACAGCAGCCTGGGGAACT and reverse GAGTCTGGGTAGGGGCAGGA; for Pref-1, forward GACACTCGAAGCTCACCTGG and reverse GGAAGGCTGGGACGGGAAAT; for Kruppel-like factor 4 (KLF4), forward GCAGTCACAAGTCCCCTCTC and reverse TAGTCACAAGTGTGGGTGGC; for Krox20, forward AGGCCGTAGACAAAATCCCAG and reverse GATACGGGAGATCCAGGGGT; for Col2a1, forward AGAACAGCATCGCCTACCTG and reverse CTTGCCCCACTTACCAGTGT; for Col10a1, forward GAAGAGCCTCGAATCACCTG and reverse ATCCTGGGCACATTATGGAA; for IL-6, forward TGTGCAATGGCAATTCTGAT and reverse TCCAGTTTGGTAGCATCCATC; for periostin, forward TGGTCACTTCACGCTCTTTG and reverse GCCACTTTGTCTCCCATGAT; for spondin 1, forward AGAGGCACCGTATGGTCAAG and reverse CGGGATGGTATGGCACTCAG; for PTX3, forward CTGCCCGCAGGTTGTGAAA and reverse AGCTTCATTGGTCTCACAGGA; for PAI-1, forward AACTACACTGAGTTCACCACCC and reverse TTCTCAAAGGGTGCAGCGAT; for hypoxia-inducible factor 1α (HIF-1α), forward CCTGCACTGAATCAAGAGGTGC and reverse CCATCAGAAGGACTTGCTGGCT; for STAT-3, forward TCCTTTCCCACTTGACCTTG and reverse CTGTAAGGCAATCCCTCTCG; for STAT-1, forward GCCTCTCATTGTCACCGAAGAAC and reverse TGGCTGACGTTGGAGATCACCA; for TNF, forward GGAGGCAACAAGGTAGAGAGG and reverse CACAGCCTTCCTCACAGAGC; for MMP-13, forward AGTTTCTTTATGGTCCAGGCGA and reverse CCTCGGAGACTGGTAATGGC; for IL-1 receptor antagonist (IL-1Ra), forward GCAAGATGCAAGCCTTCAGAATC and reverse TGGATGCCCAAGAACACACT; for cyclooxygenase 2 (COX-2), forward GCGACATACTCAAGCAGGAGCA and reverse AGTGGTAACCGCTCAGGTGTTG; for MMP-3, forward CGATGATGAACGATGGACAG and reverse AGCCTTGGCTGAGTGGTAGA; for MMP-9, forward CATTCGCGTGGATAAGGAGT and reverse TCACACGCCAGAAGAATTTG; for tissue inhibitor of metalloproteinases 1 (TIMP-1), forward GCATCTGGCATCCTCTTGTT and reverse CCTTATGACCAGGTCCGAGT; for TIMP-2, forward TTCCGGGAATGACATCTATGG and reverse GGGCCGTGTAGATAAACTCGAT; for IL-1α, forward AGTGAGCTGACCCAGCAGAT and reverse CAGGGGCTGTGTTTCTTCTC; for IL-1β, forward CCCTATGGAGATGACGGAGA and reverse CTGTCTGCTGGTGGAGTTCA; for TIMP-3, forward GAGTGAGCTCGGACTGTAGC and reverse TTTGGCCCGGATCACGATG; for HIF-2α, forward CAAGCTGAAGCTAAAGCGGC and reverse TTGGGTGAATTCATCGGGGG; for -326 to 257 bp, forward GAAAAAACTCAGGTCAGAAC

and reverse AAGAATCACAACTAGGAAGG; and for −89 to 81 bp, forward GTGGGATTTTCCCATGAGTC and reverse GCTCCAGAGCAGAATGAGC.

Cytokine quantification. The levels of granulocyte–macrophage colony-stimulating factor, interferon-γ (IFNγ), IL-1β, IL-2, IL-4, IL-5, IL-6, IL-10, IL-17, and TNF were analyzed in the supernatants of undifferentiated confluent ADSC cultures with a bead-based Analyte Detection System for quantitative detection by flow cytometry according to the recommendations of the manufacturer (eBioscience). Levels of IL-6 and periostin were measured by enzyme-linked immunosorbent assay according to the recommendations of the manufacturer (R&D Systems).

Western blot analysis. Cell extracts of stimulated or unstimulated ADSC cultures were prepared using 1× Laemmli buffer (Bio-Rad). Briefly, cells were washed twice with ice-cold PBS and snap-frozen with liquid nitrogen. Afterward, lysates were boiled for 5 minutes and centrifuged. Cell extracts from ADSCs transfected with periostin shRNA expression plasmid were prepared in Frackelton lysis buffer containing protease inhibitor cocktail. The protein content was measured by the Bradford method. Ten micrograms of protein was separated by sodium dodecyl sulfate–polyacrylamide gel electrophoresis on a 10% acrylamide gel. Semidry immunoblotting was carried out with rabbit anti-mouse STAT-3 or phospho–STAT-3 antibody (Cell Signaling Technology), rabbit anti-mouse periostin, Fra-1 antibody (Santa Cruz Biotechnology), or mouse anti-mouse β-actin antibody (Sigma-Aldrich).

Chromatin immunoprecipitation (ChIP). A ChIP assay was performed using a ChIP-IT Express kit (Active Motif). For immunoprecipitation, rabbit anti-mouse Fra-1 antibody (N-20; Santa Cruz Biotechnology) and isotype rabbit IgG antibody (Vector) as a negative control were used.

Statistical analysis. Data are shown as the mean ± SEM. The mean values from 2 groups were compared by unpaired *t*-test using GraphPad Prism software. For comparisons of more than 2 groups, one-way analysis of variance with a nonparametric post-test was performed.

RESULTS

Improved protection against collagenase-induced OA by ADSCs overexpressing Fra-1. The protective effect of ADSCs derived from 8-week-old Fra-1–transgenic mice against collagenase-induced OA was compared to that of ADSCs from wild-type mice (Figure 1). Histologic analysis of cartilage damage indicated that the protective effect of ADSCs on cartilage was greater in mice that received Fra-1–transgenic mouse ADSCs than in those that received wild-type mouse cells. Collagenase injection induced significant OA-related cartilage damage in mice, as shown by an increase in OARSI scores. OARSI scores were slightly decreased in mice that received an injection of wild-type ADSCs. Most importantly, injection with Fra-1–transgenic mouse ADSCs significantly reduced OARSI scores in mice with OA, to levels virtually indistinguishable from those in mice without OA (Figures 1B and C).

The protective effect of Fra-1–transgenic mouse ADSCs was further confirmed by quantifying the number of empty lacunae in the cartilage, which was reduced in mice injected with wild-type mouse ADSCs, and further decreased in mice injected with Fra-1–transgenic mouse ADSCs (Figure 1D). Both wild-type and Fra-1–transgenic mouse ADSCs reduced TUNEL staining to normal levels in the knee joints of mice with OA. This indicates that the decrease in empty lacunae after injection with wild-type or Fra-1–transgenic mouse ADSCs was likely due, at least partially, to an ADSC-triggered decrease in OA-related chondrocyte apoptosis observed after the injection of ADSCs (Figures 1E and F). However, TUNEL staining did not reveal differences in chondrocyte apoptosis between OA joints treated with wild-type ADSCs and those treated with Fra-1–transgenic mouse ADSCs, indicating that Fra-1–transgenic mouse ADSCs may not primarily act via influencing chondrocyte cell death. We also investigated potential changes in the subchondral bone in response to OA induction and ADSC administration. However, we did not observe significant formation of osteophytes or thickening of the subchondral bone after OA induction, with injection of either vehicle or ADSCs (Figure 1G and Supplementary Figure 1A, available on the *Arthritis & Rheumatology* web site at http://onlinelibrary.wiley.com/doi/10.1002/art.39425/abstract). Taken together, these data suggest that ADSCs that overexpress Fra-1 have a higher potential to ameliorate OA-related cartilage degeneration than wild-type ADSCs.

Increased number of adipogenic progenitors in ADSCs from Fra-1–transgenic mice. Fra-1–transgenic mice exhibit lipodystrophy, which worsens with age (14). Therefore, we hypothesized that the progenitor population of ADSCs isolated from Fra-1–transgenic mice may be different than ADSCs from wild-type mice. To analyze SVFs of the Fra-1–transgenic mouse ADSC population, (CD45−, TER119−), CD31−, CD29+, CD34+, Sca-1+, and CD24+ cells were isolated from the fat pads of wild-type and Fra-1–transgenic mice and quantified by FACS. This subpopulation is believed to represent early adipocyte progenitor cells in white adipose tissue (24). As expected, their absolute number was decreased in the fat pads of Fra-1–transgenic mice (data not shown). However, the percentage of adipogenic progenitors in SVFs from 8-week-old Fra-1–transgenic mice was almost twice as high as that in SVFs from wild-type littermate controls (Figures 2A and B).

In order to investigate whether Fra-1 overexpression affects the differentiation potential of fat-derived progenitor cells, we studied adipogenic and chondrogenic differentiation of ADSCs isolated from the fat pads of wild-type and Fra-1–transgenic mice. After 14 days of adipogenic differentiation in vitro, oil red O

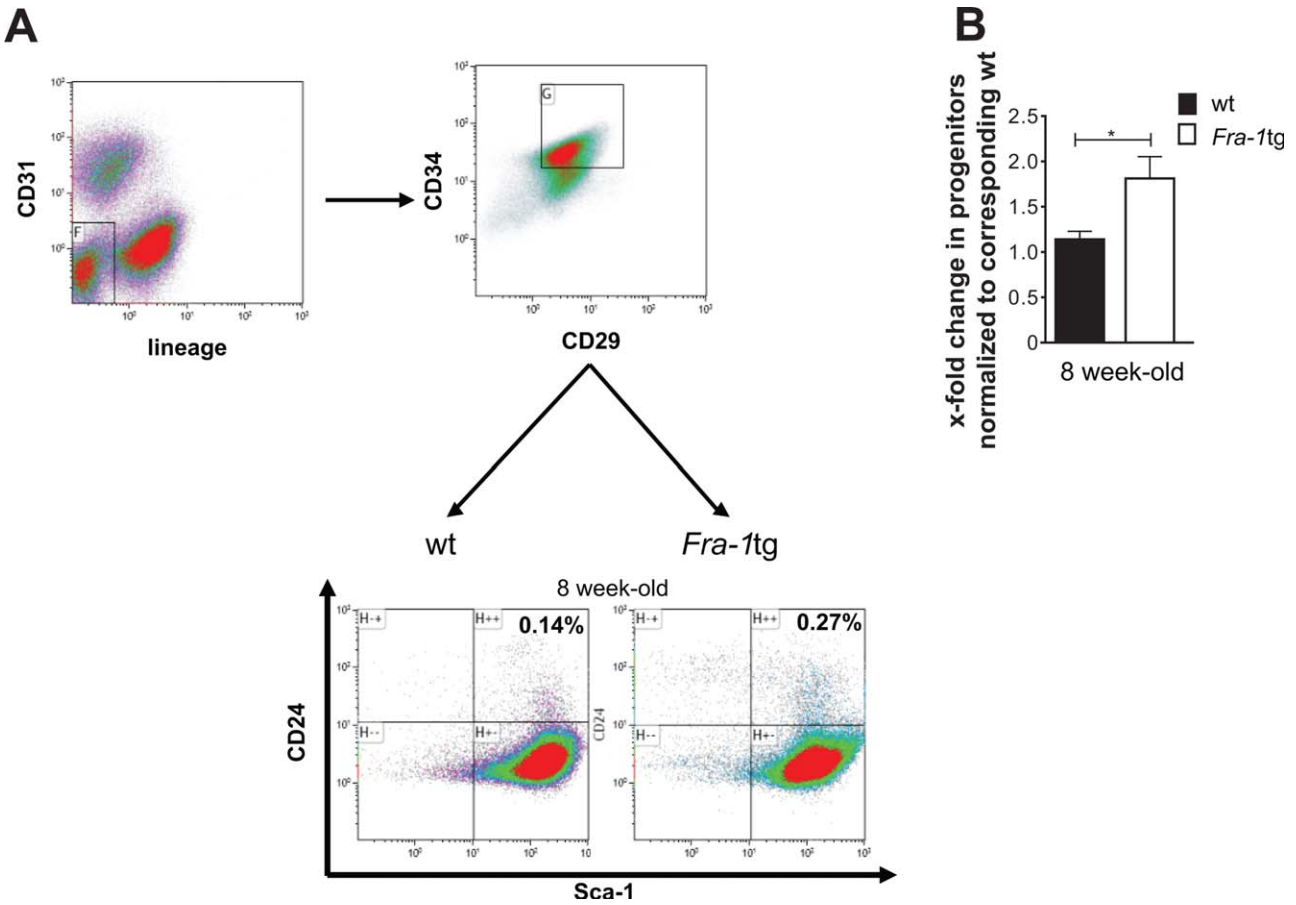

Figure 2. Increased number of adipogenic progenitors in the fat pads of 8-week-old Fra-1–transgenic (Fra-1Tg) mice. **A,** Dot plots showing representative fluorescence-activated cell sorting staining profiles, and gating with lineage-negative (CD45−, TER119−), CD31−, CD29+, CD34+, Sca-1+, and CD24+ cells as adipogenic progenitor markers of stromal vascular fractions (SVFs), in 8-week-old wild-type (WT) and Fra-1–transgenic mice. **B,** Quantification of adipogenic progenitors in Fra-1–transgenic mouse SVFs normalized to SVFs from 8-week-old wild-type mice. Bars show the mean ± SEM (n = 6 mice per group). $* = P < 0.05$.

staining indicated impaired adipogenesis of Fra-1–transgenic compared to wild-type mouse ADSCs (Figure 3A). Blockade of adipogenesis was confirmed by analyzing the levels of messenger RNA (mRNA) for adipogenic marker genes during the course of adipocyte differentiation (Figure 3B). Overexpression of Fra-1 was associated with significantly decreased C/EBPα and PPARγ2 mRNA levels and a tendency toward reduced GLUT-4 gene expression (Figure 3B). In addition, the expression of marker genes for adipogenic progenitors, such as Pref-1, C/EBPβ, Krox20, and KLF4, was increased in Fra-1–transgenic mouse ADSCs on day 0, probably reflecting the higher proportion of adipocyte progenitors in Fra-1–transgenic mice (Figure 3B and Supplementary Figure 1B, available on the *Arthritis & Rheumatology* web site at http://onlinelibrary.wiley.com/doi/10.1002/art.39425/abstract).

In contrast to these differences in adipogenic differentiation, we did not observe a difference in the chondrogenic potential between wild-type mouse and Fra-1–transgenic mouse ADSCs, as shown by similar Col2a1 and Col10a1 mRNA levels after chondrogenic differentiation in vitro (see Supplementary Figures 1C and D, available on the *Arthritis & Rheumatology* web site at http://onlinelibrary.wiley.com/doi/10.1002/art.39425/abstract). Finally, analysis of apoptosis revealed no difference between wild-type and Fra-1–transgenic mouse ADSCs (Figure 3C). These findings suggest that enhanced protection against OA by ADSCs that overexpress Fra-1 may be mediated by increased numbers of adipogenic progenitors in Fra-1–transgenic mouse ADSC fractions.

No increased protection against OA with progenitor-enriched ADSCs. To test the above hypothesis, SVFs from 8-week-old wild-type mice were either

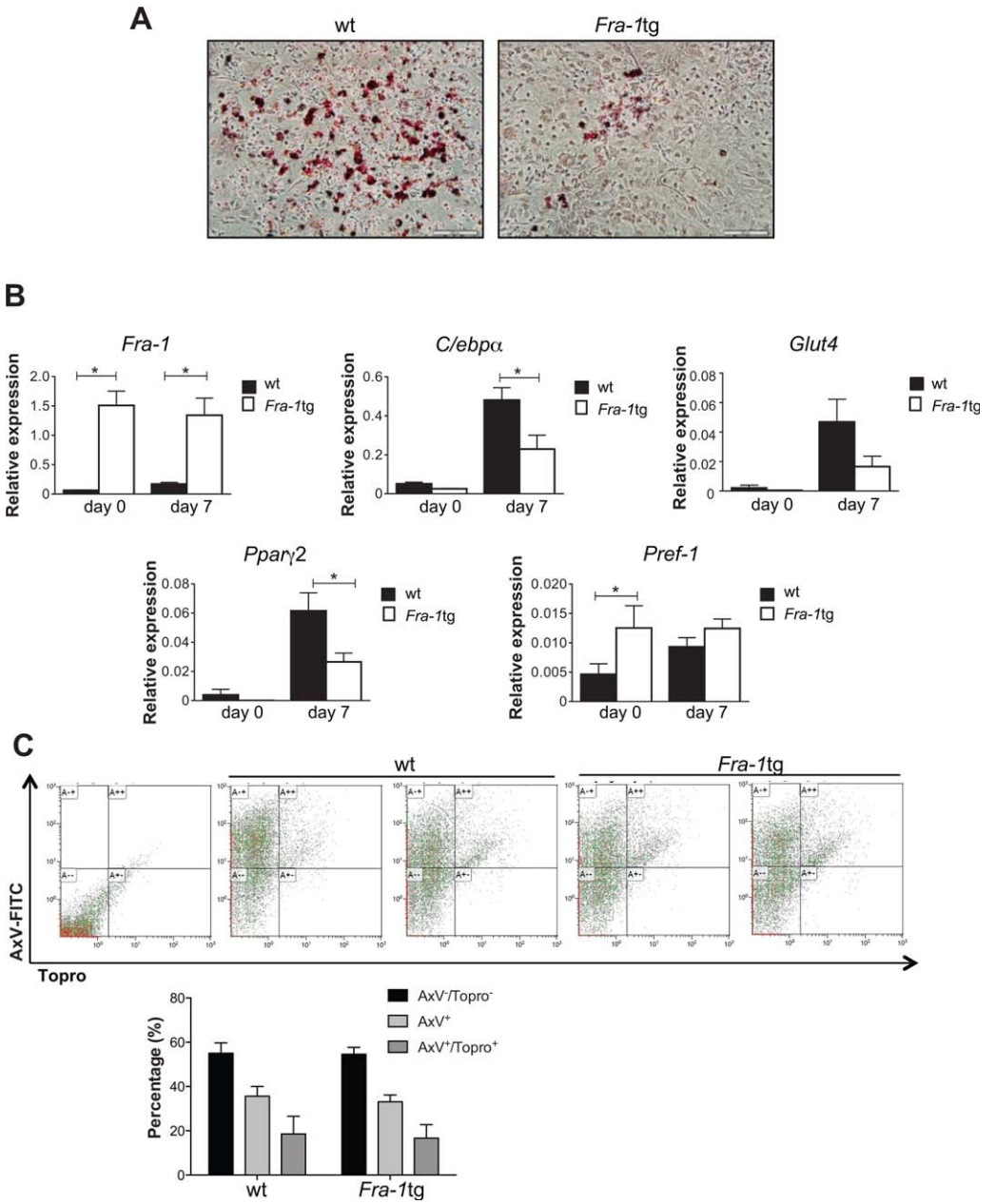

Figure 3. Decreased adipogenic potential of Fra-1–transgenic (Fra-1Tg) mouse adipose-derived stromal cells (ADSCs) in vitro. **A,** Oil red O staining of ADSCs from wild-type (WT) and Fra-1–transgenic mice, after 14 days of adipogenic differentiation. **B,** Relative expression levels of mRNA for Fra-1 and the adipocyte marker genes CCAAT/enhancer binding protein α (C/EBPα), glucose transporter 4 (GLUT-4), peroxisome proliferator–activated receptor γ2 (PPARγ2), and Pref-1 on days 0 and 7 of in vitro adipogenic differentiation of wild-type or Fra-1–transgenic mouse ADSCs. Bars show the mean ± SEM (n = 4 mice per group). **C,** Representative quadrant dot plot analysis showing fluorescence-activated cell sorting staining profiles of unstained wild-type mouse ADSCs and stained wild-type or Fra-1–transgenic mouse ADSCs at passage 1. Gating and quantification were performed using fluorescein isothiocyanate (FITC)–conjugated annexin V (AxV) and TO-PRO-3 (Topro). Bars show the mean ± SEM (n = 3 mice per group). * = $P < 0.05$.

directly cultured until the end of passage 1 (nonsorted ADSC pool) or enriched for adipogenic progenitor cells prior to cultivation. For enrichment of adipogenic progenitors, cells were sorted by FACS for lineage-negative (CD45−, TER119−), CD31−, CD29+, CD34+, Sca-1+ cells and cultured until the end of passage 1 (sorted ADSC pool). Both ADSC pools were then injected into the knee joints 7 days after the induction of OA (Figure

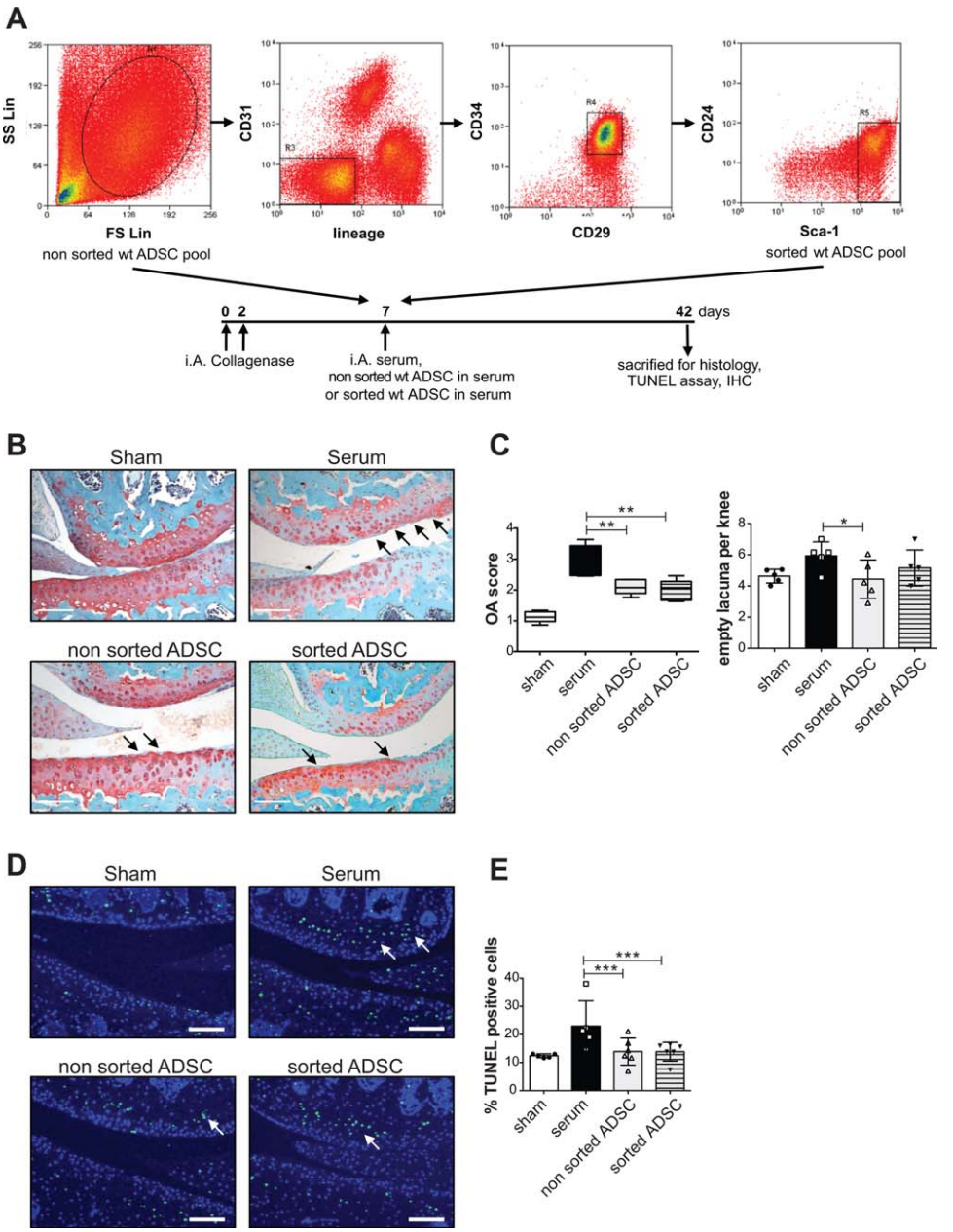

Figure 4. Enrichment of adipogenic progenitors does not increase the protective effects of adipose-derived stromal cells (ADSCs) on collagenase-induced osteoarthritis (OA). **A,** Schematic illustration of the schedule of induction of collagenase-induced OA in mice and treatment with nonsorted or sorted ADSCs. Stromal vascular fractions isolated from 8-week-old wild-type (WT) mice were cultured either as nonsorted wild-type ADSCs or after enrichment for adipogenic progenitors by fluorescence-activated cell sorting for lineage-negative (CD45−, TER119−), CD31−, CD29+, CD34+, and Sca-1+ cells (sorted ADSCs). SS Lin = side scatter lineage; FS Lin = forward scatter lineage; IA = intraarticular; IHC = immunohistochemical analysis. **B,** Safranin O–fast green–stained frontal knee joint sections from control mice without OA (sham) and mice with OA that were injected with serum, nonsorted wild-type ADSCs, or sorted wild-type ADSCs. **Arrows** indicate cartilage lesions. **C,** Quantification of cartilage damage and mean number of empty chondrocyte lacunae per knee joint in control mice without OA and mice with OA treated as indicated. Data in the left panel are shown as box plots. Each box represents the 25th to 75th percentiles. Lines inside the boxes represent the mean. Lines outside the boxes represent the 10th and 90th percentiles. Bars in the right panel show the mean ± SEM. Symbols represent individual mice (n = 5 mice per group). **D** and **E,** TUNEL staining (**D**) and mean percentage of TUNEL-positive cells (**E**) in knee joint sections from control mice without OA and mice with OA that were injected with serum, nonsorted wild-type ADSCs, or sorted wild-type ADSCs. **Arrows** indicate TUNEL-positive cells. Bars in **E** show the mean ± SEM. Symbols represent individual mice (n = 5 mice per group). Bars in **B** and **D** = 100 μm. * = $P < 0.05$; ** = $P < 0.001$; *** = $P < 0.0001$.

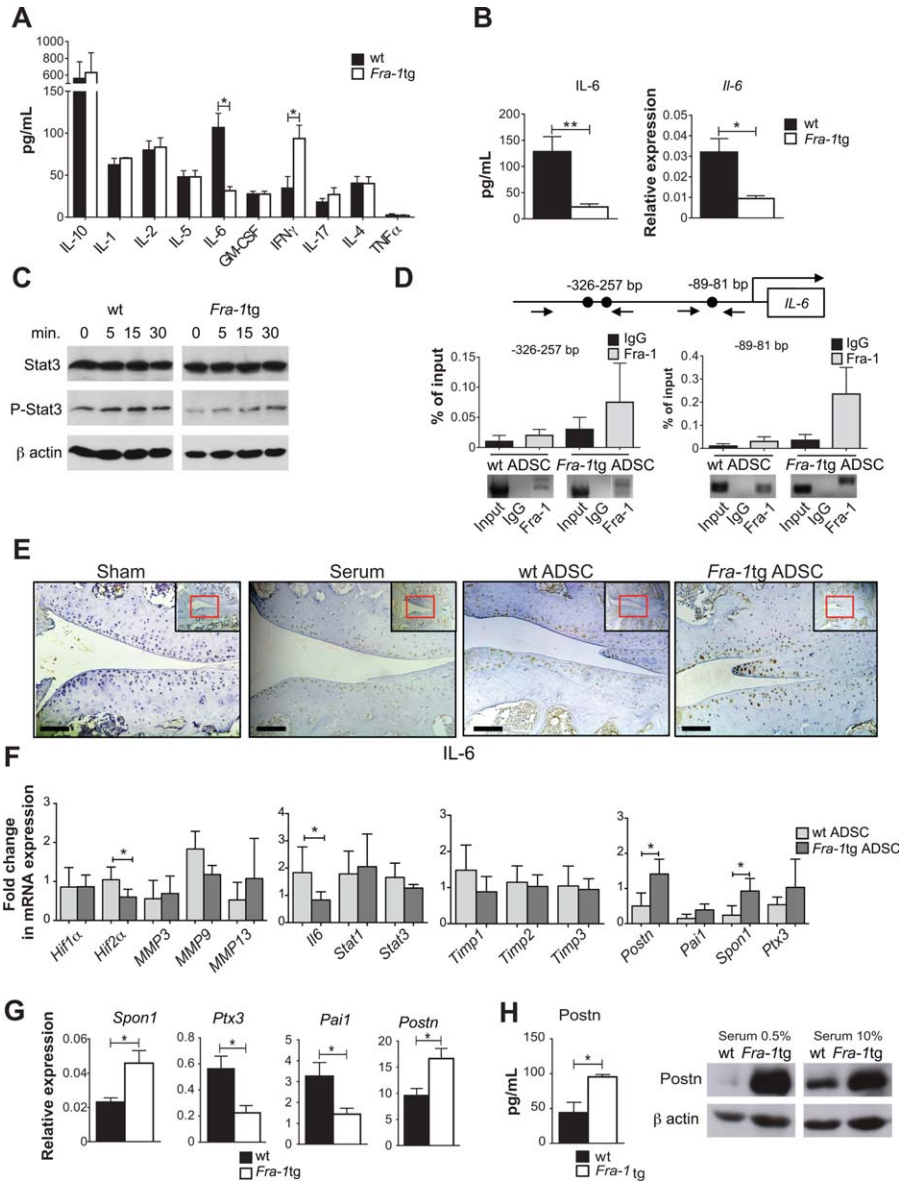

Figure 5. Decreased interleukin-6 (IL-6) secretion and modified expression of extracellular matrix homeostasis regulators in Fra-1–transgenic (Fra-1Tg) mouse adipose-derived stromal cells (ADSCs). **A,** Levels of cytokines released into the medium by cultured wild-type (WT) and Fra-1–transgenic mouse ADSCs. GM-CSF = granulocyte–macrophage colony-stimulating factor; IFNγ = interferon-γ; TNF = tumor necrosis factor. **B,** IL-6 mRNA and protein levels in wild-type and Fra-1–transgenic mouse ADSCs. **C,** Western blot analysis of STAT-3, phospho–STAT-3, and β-actin protein levels in wild-type and Fra-1–transgenic mouse ADSCs stimulated with leptin (n = 2 mice per group). **D,** Chromatin immunoprecipitation of Fra-1 binding to the IL-6 promoter. **Arrows** indicate primer-amplifying fragments for the TRE elements. Real-time polymerase chain reaction analyses and loading of the gel are shown (n = 2). **E,** Immunohistochemical staining for IL-6 in knee joint sections from control mice without OA and mice with OA that were injected with serum, wild-type mouse ADSCs, or Fra-1–transgenic mouse ADSCs. The larger panels are higher-magnification views of the boxed areas in the **insets**. Original magnification $\times$ 20; $\times$ 10 in **insets**. Bars = 100 μm. **F,** Fold change in expression levels of mRNA for catabolic and anabolic factors in knee joints from mice with OA that were injected with wild-type or Fra-1–transgenic mouse ADSCs. HIF-1α = hypoxia-inducible factor 1α; MMP-3 = matrix metalloproteinase 3; TIMP-1 = tissue inhibitor of metalloproteinases 1. **G,** Relative expression levels of mRNA for spondin 1 (Spon1), pentraxin 3 (PTX3), plasminogen activator inhibitor 1 (PAI-1), and periostin (Postn) in wild-type and Fra-1–transgenic mouse ADSCs. **H,** Protein levels of periostin in conditioned medium (left) and cell lysates of wild-type and Fra-1–transgenic mouse ADSCs (right). Values in **A, B, D, F, G,** and **H** are the mean $\pm$ SEM (n = 2–4 mice per group in **A,** 4 mice per group in **B** and **G,** 2 mice per group in **D,** 6 mice per group in **F,** and 3 mice per group in **H**). $* = P < 0.05$; $** = P < 0.001$.

4A). Histologic analyses, including OA scores and quantification of empty lacunae and TUNEL-positive articular chondrocytes, revealed that nonsorted and sorted wild-type ADSCs had similar protective effects against collagenase-induced OA (Figures 4B–E). These data suggest that enrichment of adipogenic progenitors in ADSC fractions does not improve the chondroprotective potential of ADSCs in OA. Fra-1 overexpression therefore appears necessary for mediating the protective effect of ADSCs in OA.

Molecular characteristics of ADSCs overexpressing Fra-1. To elucidate the molecular mechanisms mediating the improved protective effect of Fra-1–overexpressing ADSCs in OA, cytokine secretion by wild-type and Fra-1–transgenic mouse ADSCs were profiled by FACS bead-based cytokine array. As shown in Figure 5A, IFNγ secretion into the medium was up-regulated, while secretion of IL-6, a proinflammatory cytokine, was decreased in Fra-1–transgenic mouse ADSC cultures. Decreased IL-6 secretion by Fra-1–transgenic mouse ADSCs was confirmed by enzyme-linked immunosorbent assay (ELISA). Furthermore, IL-6 mRNA levels were significantly lower in Fra-1–transgenic mouse ADSCs compared to wild-type cells (Figure 5B). Moreover, wild-type and Fra-1–transgenic mouse ADSCs treated with LPS had similar TNF, IL-1α, and IL-1β mRNA levels (Figure 6C).

IL-6 expression can be induced by leptin, which is abundantly present in OA. Therefore, we investigated the induction of the IL-6 signaling pathway in ADSCs after stimulation with leptin. Leptin-triggered STAT-3 phosphorylation, a central event in IL-6 signal transduction, was effectively altered in Fra-1–transgenic mouse ADSCs compared to wild-type mouse ADSCs (Figure 5C). These data suggest that Fra-1 regulates IL-6 expression and secretion in ADSCs. Interestingly, the IL-6 promoter harbors 2 TPA DNA response elements (TRE; 5′-TGAG/CTCA-3′), which represent consensus binding sites for AP-1 transcription factors (Figure 5D). This prompted us to examine whether IL-6 is a direct target of Fra-1 in ADSCs. Indeed, Fra-1 can directly bind to the IL-6 promoter, indicating that Fra-1 directly modulates IL-6 transcription (Figure 5D).

Molecular expression patterns of the joints of mice with OA that received ADSCs. We next analyzed the molecular expression patterns of the joints of mice with OA that received wild-type or Fra-1–transgenic mouse ADSCs in vivo. Despite the fact that immunohistochemical staining revealed increased IL-6 protein levels in the knee joints of mice with OA, we were not able to detect overt differences in IL-6 expression between vehicle-treated or ADSC-treated joints by immunohistochemistry (Figure 5E). Because of the limitations of immunohistochemistry in quantifying changes in marker expression, we undertook comparative gene expression studies of the knee joints of mice with OA treated with wild-type or Fra-1–transgenic mouse ADSCs. We found that not only expression of mRNA for IL-6, but also expression of the proinflammatory mediator PTX3 and of PAI-1 were significantly decreased in mice that received Fra-1–transgenic compared to wild-type mouse ADSCs (Figure 5F). We also found a slight decrease in HIF-2α expression, while expression of HIF-1α, MMPs (MMP-3, MMP-9, and MMP-13), TIMPs 1–3, and TGFβ was not affected (Figure 5F and data not shown). In contrast, levels of the matrix proteins periostin and spondin 1 were significantly increased in the joints of mice with OA treated with Fra-1–transgenic mouse ADSCs (Figure 5F). Consistent with these findings, Fra-1–transgenic mouse ADSCs also exhibited increased periostin and spondin 1 mRNA levels compared to wild-type ADSCs in vitro, whereas PTX3 and PAI-1 mRNA levels were decreased (Figure 5G).

In order to investigate ADSC gene expression under inflammatory conditions, wild-type and Fra-1–transgenic mouse ADSCs were stimulated with LPS. Fra-1–transgenic mouse ADSCs exhibited significantly milder induction of COX-2 gene expression after LPS stimulation, while the expression levels of TIMPs 1–3, IL-1Ra, and MMP-13 did not significantly differ between LPS-treated wild-type and Fra-1–transgenic mouse ADSCs (Figures 6A and B).

Periostin has been described to regulate chondrocyte survival. Here we showed that periostin expression was increased at the mRNA and protein levels in Fra-1–transgenic mouse ADSCs and in knee joints injected with Fra-1–transgenic mouse ADSCs (Figures 5F–H). In order to investigate whether periostin may mediate Fra-1–triggered protective effects against OA-related cartilage damage, periostin was knocked down in Fra-1–transgenic mouse ADSCs (Supplementary Figure 2, on the *Arthritis & Rheumatology* web site at http://onlinelibrary.wiley.com/doi/10.1002/art.39425/abstract). However, the knockdown of periostin did not reverse the chondroprotective effect of Fra-1–transgenic mouse ADSCs in collagenase-induced OA (Figure 6D), suggesting that periostin alone is not sufficient to conduce the protective effect of Fra-1–transgenic mouse ADSCs and that a more comprehensive change in ADSC gene expression, as indicated above, is necessary to mediate the protective role of Fra-1–transgenic mouse ADSCs on the articular cartilage. Taken together, these results demonstrate that decreased proinflammatory IL-6 and PTX3 expression along with increased spondin 1 and peri-

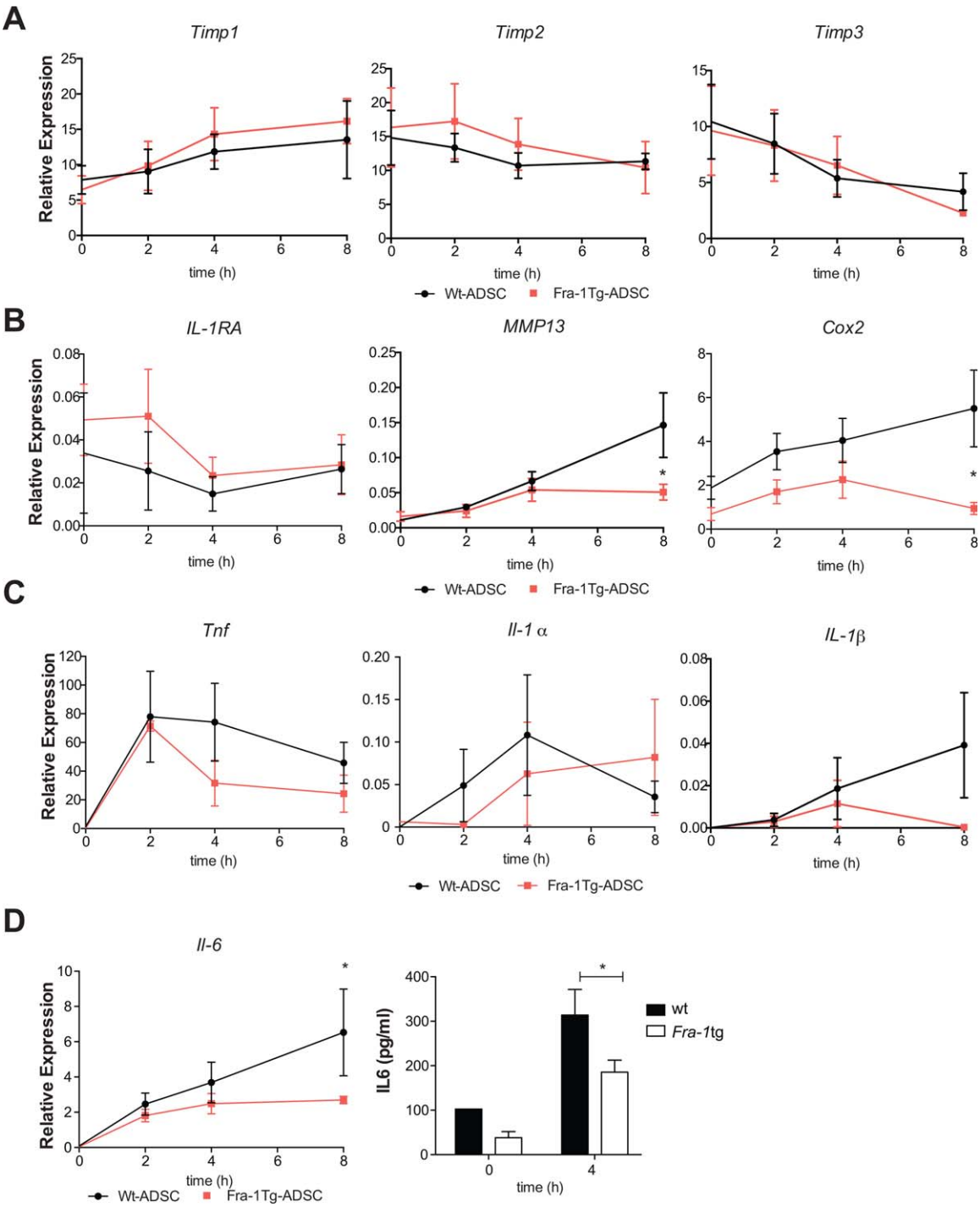

Figure 6. Decreased levels of cyclooxygenase 2 (COX-2) and interleukin-6 (IL-6) mRNA during inflammatory response in Fra-1–transgenic (Fra-1Tg) mouse adipose-derived stromal cells (ADSCs). **A** and **B,** Relative expression levels of mRNA for tissue inhibitors of metalloproteinases (TIMPs) 1–3 (**A**) and IL-1 receptor antagonist (IL-1Ra), matrix metalloproteinase 13 (MMP-13), and COX-2 (**B**) in wild-type and Fra-1–transgenic mouse ADSCs at the indicated time points after stimulation with lipopolysaccharide (LPS) (n = 3 mice per group). **C,** Relative expression levels of mRNA for the inflammatory marker genes tumor necrosis factor (TNF), IL-1α, and IL-1β at the indicated time points after stimulation of wild-type and Fra-1–transgenic mouse ADSCs with LPS (n = 3 mice per group). **D,** Relative expression levels of IL-6 mRNA and protein in cells and supernatants at the indicated time points after stimulation of wild-type and Fra-1–transgenic mouse ADSCs with LPS (n = 3 mice per group). Values are the mean ± SEM. $* = P < 0.05$, wild-type versus Fra-1–transgenic mouse ADSCs.

ostin expression in Fra-1–transgenic mouse ADSCs may essentially mediate the beneficial effect of Fra-1–transgenic mouse ADSCs on cartilage degradation in OA.

DISCUSSION

Several studies have demonstrated that MSCs can be used to treat OA. In rabbit and mouse studies, intraarticular injection of stem cells from adipose tissue ameliorated collagenase-induced and surgically induced OA (10,11). In fact, wild-type ADSCs have intrinsic antiinflammatory effects on chondrocytes and synoviocytes (25). Since secondary synovial inflammation in OA is believed to be a major contributor to disease burden, fostering antiinflammatory pathways in ADSCs might improve the therapeutic value of these cells. Furthermore, ADSCs decreased the tendency of OA chondrocytes to become fibrotic or hypertrophic (26). In addition to their primary effect on cartilage, wild-type ADSCs may affect other joint tissues, such as the synovial membrane, the ligaments, and the subchondral bone (10,26). Modulating the secretion of extracellular matrix proteins from ADSCs, which could affect the turnover of cartilage and other joint tissues, may therefore further stimulate the chondroprotective effects of ADSCs in OA.

In this study, we considered the AP-1 transcription factor Fra-1 as a potential candidate to modulate the effect of ADSCs on OA progression since it is involved in both bone and fat differentiation as well as in the regulation of inflammation (12). Indeed, the transcription factor Fra-1 regulates MGP and (13) C/EBPα transcription (14). The present study demonstrates that Fra-1 overexpression can enhance the protective effect of ADSCs on cartilage integrity during experimental OA in mice. We first hypothesized that the increased numbers of adipogenic progenitor cells observed in ADSC fractions from Fra-1–transgenic mice might be the mechanism by which Fra-1–transgenic mouse ADSCs provided better protection against OA-mediated cartilage damage compared to wild-type mouse ADSCs. However, an increase in adipogenic progenitor numbers was not sufficient to modulate ADSC-mediated cartilage protection in OA. Thus, injection of wild-type ADSCs enriched for adipogenic progenitors did not augment the level of protection when compared to the nonsorted ADSCs cells. This observation is supported by previous studies showing that ADSCs from different fat tissue samples with different quantities of progenitors have similar chondroprotective properties in OA (25). Therefore, increased Fra-1 expression mediated the beneficial effect of ADSCs in OA.

Several in vitro studies have shown that Fra-1 is highly involved in the inflammatory response of macrophages by modulating cytokines such as IL-6, TNF, and IL-1β (27–29). IL-6 plays a pivotal role in autoimmune mechanisms, in acute inflammation, and in the development of chronic inflammatory states through the IL-6R/STAT-3 pathway (30,31). Most importantly, in mouse models of OA, IL-6 promotes cartilage destruction by inducing the expression of catabolic genes (32). Our analysis of the cytokine secretion pattern of ADSCs that overexpress Fra-1 by multiplex bead-based immunoassay or ELISA revealed significantly reduced secretion of IL-6 from Fra-1–transgenic mouse ADSCs compared to wild-type cells. This effect was based on a Fra-1–dependent decrease in the levels of IL-6 mRNA, since we showed that Fra-1 directly binds to the promoter of IL-6, and Fra-1–transgenic mouse ADSCs exhibit reduced levels of IL-6 mRNA. Consistent with these findings, STAT-3 signaling was also reduced in Fra-1–transgenic mouse ADSCs, suggesting lower levels of autocrine IL-6 signaling in Fra-1–transgenic mouse ADSCs compared to wild-type cells. Interestingly, even wild-type mouse ADSCs have been shown to exert antiinflammatory effects on chondrocytes and synoviocytes in vitro, including the suppression of IL-6 mRNA expression (25). In this study, we demonstrate that total IL-6 mRNA levels in OA joints were reduced even further after injection of Fra-1–transgenic mouse ADSCs than after injection of wild-type mouse ADSCs, suggesting that the reduction in IL-6 levels may represent a pivotal contribution to ADSC-dependent antiinflammatory and chondroprotective effects.

In addition to IL-6, other chemokines, such as CXCL1, CCL2, and CCL5, as well as matrix degradation enzymes have been found to be down-regulated after treatment of OA with ADSCs (25). We hypothesized that Fra-1 overexpression may additionally alter the expression and secretion of other proteins involved in cartilage metabolism in ADSCs. Interestingly, Fra-1 has been shown to directly control the expression of MGP, a secreted protein associated with calcification processes. MGP mRNA levels have been shown to be markedly increased in the long bones of Fra-1–transgenic mice (13). Moreover, Fra-1 knockdown has been demonstrated to enhance the expression of type I collagen and to down-regulate MMP-1 and MMP-13 gene expression in human lung epithelial cells (33). These examples highlight the potential of Fra-1 to regulate gene expression of secreted proteins associated with cartilage and bone homeostasis.

Although we did not observe major differences between the expression levels of MMPs or TIMPs, the expression levels of PTX3 and PAI-1, as well as those of periostin and spondin 1, were significantly altered by Fra-1 in ADSCs. Effectively, the decrease in PTX3 and

PAI-1, as well as the increase in periostin and spondin 1 in Fra-1–transgenic mouse ADSCs, could contribute to the increased protective effect of Fra-1–transgenic mouse ADSCs in OA (34). PTX3 is a mediator of inflammation (35,36), and PAI-1 is expressed by OA chondrocytes and modulates plasmin activation and degradation of the extracellular matrix (37). Expression of the extracellular matrix protein periostin is increased during fracture healing where its primary role is to promote recruitment and adhesion of chondroprogenitors and osteoprogenitors from bone marrow and blood (38). Therefore, it is tempting to speculate that the elevated secretion of periostin by Fra-1–transgenic mouse ADSCs may alone be sufficient to increase the chondroprotective effect of these cells in OA. However, siRNA-mediated knockdown of periostin in Fra-1–transgenic mouse ADSCs was not sufficient to alter the effect of these cells in ameliorating OA-induced cartilage damage. Thus, the improved protective effect of Fra-1–transgenic mouse ADSCs on cartilage integrity is probably mediated by a comprehensive change in the gene expression pattern of ADSCs, consisting of the downregulation of inflammatory genes and increased expression of extracellular matrix genes.

In summary, we demonstrated that ADSCs that overexpress Fra-1, which show a comprehensive change toward an antiinflammatory/proanabolic gene expression pattern, effectively protect against cartilage damage in experimental OA. These data provide new insights into the understanding of the best configuration of ADSCs to effectively protect against cartilage damage. Genetic modification of ADSCs may therefore emerge as a powerful tool to enhance the chondroprotective effects of these cells in OA treatment.

ACKNOWLEDGMENTS

We thank Dr. Wolfgang Baum for assistance with animal experiments and Christine Zech for great technical assistance.

AUTHOR CONTRIBUTIONS

All authors were involved in drafting the article or revising it critically for important intellectual content, and all authors approved the final version to be published. Dr. Bozec had full access to all of the data in the study and takes responsibility for the integrity of the data and the accuracy of the data analysis.

Study conception and design. Schwabe, David, Schett, Bozec.

Acquisition of data. Schwabe, Garcia, Ubieta, Hannemann, Herbort, Luther, Noël, Jorgensen, Casteilla, David, Stock, Herrmann, Schett, Bozec.

Analysis and interpretation of data. Schwabe, Garcia, Ubieta, Hannemann, Herbort, David, Schett, Bozec.

REFERENCES

1. Woolf AD, Pfleger B. Burden of major musculoskeletal conditions. Bull World Health Organ 2003;81:646–56.
2. Lawrence RC, Felson DT, Helmick CG, Arnold LM, Choi H, Deyo RA, et al, for the National Arthritis Data Workgroup. Estimates of the prevalence of arthritis and other rheumatic conditions in the United States: part II. Arthritis Rheum 2008;58:26–35.
3. Loeser RF, Goldring SR, Scanzello CR, Goldring MB. Osteoarthritis: a disease of the joint as an organ [review]. Arthritis Rheum 2012;64:1697–707.
4. Goldring MB, Goldring SR. Osteoarthritis. J Cell Physiol 2007;213:626–34.
5. Goldring MB, Marcu KB. Cartilage homeostasis in health and rheumatic diseases. Arthritis Res Ther 2009;11:224.
6. Hunziker EB. Articular cartilage repair: basic science and clinical progress. A review of the current status and prospects. Osteoarthritis Cartilage 2002;10:432–63.
7. Hunter DJ. Pharmacologic therapy for osteoarthritis—the era of disease modification. Nat Rev Rheumatol 2011;7:13–22.
8. Dominici M, Le Blanc K, Mueller I, Slaper-Cortenbach I, Marini F, Krause D, et al. Minimal criteria for defining multipotent mesenchymal stromal cells: the International Society for Cellular Therapy position statement. Cytotherapy 2006;8:315–7.
9. Zhu Y, Liu T, Song K, Fan X, Ma X, Cui Z. Adipose-derived stem cell: a better stem cell than BMSC. Cell Biochem Funct 2008:664–75.
10. Ter Huurne M, Schelbergen R, Blattes R, Blom A, de Munter W, Grevers LC, et al. Antiinflammatory and chondroprotective effects of intraarticular injection of adipose-derived stem cells in experimental osteoarthritis. Arthritis Rheum 2012;64:3604–13.
11. Desando G, Cavallo C, Sartoni F, Martini L, Parrilli A, Veronesi F, et al. Intra-articular delivery of adipose derived stromal cells attenuates osteoarthritis progression in an experimental rabbit model. Arthritis Res Ther 2013;15:R22.
12. Wagner EF, Eferl R. Fos/AP-1 proteins in bone and the immune system. Immunol Rev 2005;208:126–40.
13. Julien M, Khoshniat S, Lacreusette A, Gatius M, Bozec A, Wagner EF, et al. Phosphate dependent regulation of MGP in osteoblasts: role of ERK1/2 and Fra-1. J Bone Miner Res 2009;24:1856–68.
14. Luther J, Driessler F, Megges M, Hess A, Herbort B, Mandic V, et al. Elevated Fra-1 expression causes severe lipodystrophy. J Cell Sci 2011;124:1465–76.
15. Zenz R, Eferl R, Scheinecker C, Redlich K, Smolen J, Schonthaler HB, et al. Activator protein 1 (Fos/Jun) functions in inflammatory bone and skin disease. Arthritis Res Ther 2008;10:201.
16. Wagner EF. Bone development and inflammatory disease is regulated by AP-1 (Fos/Jun). Ann Rheum Dis 2010;69 Suppl 1:i86–8.
17. Jochum W, David JP, Elliott C, Wutz A, Plenk H, Matsuo K, et al. Increased bone formation and osteosclerosis in mice overexpressing the transcription factor Fra-1. Nat Med 2000;6:980–4.
18. Planat-Benard V, Silvestre JS, Cousin B, Andre M, Nibbelink M, Tamarat R, et al. Plasticity of human adipose lineage cells toward endothelial cells: physiological and therapeutic perspectives. Circulation 2004;109:656–63.
19. Puissant B, Barreau C, Bourin P, Clavel C, Corre J, Bousquet C, et al. Immunomodulatory effect of human adipose tissue-derived adult stem cells: comparison with bone marrow mesenchymal stem cells. Br J Haematol 2005;129:118–29.
20. Van der Kraan PM, Vitters EL, van Beuningen HM, van de Putte LB, van den Berg WB. Degenerative knee joint lesions in mice after a single intra-articular collagenase injection: a new model of osteoarthritis. J Exp Pathol (Oxford) 1990;71:19–31.
21. Van Osch GJ, van der Kraan PM, van den Berg WB. Site-specific cartilage changes in murine degenerative knee joint disease

induced by iodoacetate and collagenase. J Orthop Res 1994;12: 168–75.
22. Van Osch GJ, Blankevoort L, van der Kraan PM, Janssen B, Hekman E, Huiskes R, et al. Laxity characteristics of normal and pathological murine knee joints in vitro. J Orthop Res 1995; 13:783–91.
23. Glasson SS, Chambers MG, Van Den Berg WB, Little CB. The OARSI histopathology initiative—recommendations for histological assessments of osteoarthritis in the mouse. Osteoarthritis Cartilage 2010;18 Suppl 3:S17–23.
24. Rodeheffer MS, Birsoy K, Friedman JM. Identification of white adipocyte progenitor cells in vivo. Cell 2008;135:240–9.
25. Manferdini C, Maumus M, Gabusi E, Piacentini A, Filardo G, Peyrafitte JA, et al. Adipose-derived mesenchymal stem cells exert antiinflammatory effects on chondrocytes and synoviocytes from osteoarthritis patients through prostaglandin E_2. Arthritis Rheum 2013;65:1271–81.
26. Maumus M, Manferdini C, Toupet K, Peyrafitte JA, Ferreira R, Facchini A, et al. Adipose mesenchymal stem cells protect chondrocytes from degeneration associated with osteoarthritis. Stem Cell Res 2013;11:834–44.
27. Morishita H, Saito F, Kayama H, Atarashi K, Kuwata H, Yamamoto M, et al. Fra-1 negatively regulates lipopolysaccharide-mediated inflammatory responses. Int Immunol 2009;21:457–65.
28. Luo YP, Zhou H, Krueger J, Kaplan C, Liao D, Markowitz D, et al. The role of proto-oncogene Fra-1 in remodeling the tumor microenvironment in support of breast tumor cell invasion and progression. Oncogene 2010;29:662–73.
29. Wang Q, Ni H, Lan L, Wei X, Xiang R, Wang Y. Fra-1 protooncogene regulates IL-6 expression in macrophages and promotes the generation of M2d macrophages. Cell Res 2010;20:701–12.
30. Fonseca JE, Santos MJ, Canhao H, Choy E. Interleukin-6 as a key player in systemic inflammation and joint destruction. Autoimmun Rev 2009;8:538–42.
31. Pedersen BK, Brandt C. The role of exercise-induced myokines in muscle homeostasis and the defense against chronic diseases. J Biomed Biotechnol 2010;2010:520258.
32. Ryu JH, Yang S, Shin Y, Rhee J, Chun CH, Chun JS. Interleukin-6 plays an essential role in hypoxia-inducible factor 2α–induced experimental osteoarthritic cartilage destruction in mice. Arthritis Rheum 2011;63:2732–43.
33. Rajasekaran S, Vaz M, Reddy SP. Fra-1/AP-1 transcription factor negatively regulates pulmonary fibrosis in vivo. PLoS One 2012;7:e41611.
34. Palmer GD, Piton AH, Thant LM, Oliveira SM, D'Angelo M, Attur MG, et al. F-spondin regulates chondrocyte terminal differentiation and endochondral bone formation. J Orthop Res 2010;28:1323–9.
35. Ortega-Hernandez OD, Bassi N, Shoenfeld Y, Anaya JM. The long pentraxin 3 and its role in autoimmunity. Semin Arthritis Rheum 2009;39:38–54.
36. Daigo K, Mantovani A, Bottazzi B. The yin-yang of long pentraxin PTX3 in inflammation and immunity. Immunol Lett 2014; 161:38–43.
37. Yeh CC, Chang HI, Chiang JK, Tsai WT, Chen LM, Wu CP, et al. Regulation of plasminogen activator inhibitor 1 expression in human osteoarthritic chondrocytes by fluid shear stress: role of protein kinase Cα. Arthritis Rheum 2009;60:2350–61.
38. Nakazawa T, Nakajima A, Seki N, Okawa A, Kato M, Moriya H, et al. Gene expression of periostin in the early stage of fracture healing detected by cDNA microarray analysis. J Orthop Res 2004;22:520–5.